A 1D CIRCULATION MODEL AS BOUNDARY CONDITION FOR A 3D SIMULATION OF A PUMPING HUMAN VENTRICLE

M. Reik*, G. Meyrowitz**, M. Schwarz**, S. Donisi*, T. Schenkel* and U. Kiencke**

* Institute for Fluid Mechanics, University of Karlsruhe (TH), Germany
** Institute of Industrial Information Technology, University of Karlsruhe (TH), Germany

reik@isl.mach.uni-karlsruhe.de

Abstract: The Institute for Fluid Mechanics, University of Karlsruhe, is developing a model for 3D simulations of a pumping human heart. The movement is prescribed in the simulations by a model based on Magnetic Resonance Images. Like in other biomedical simulations boundary conditions are a very critical part of the simulations. Due to the assumed incompressibility of blood the calculated fluid structure is not dependent on the pressure level. But to determine the efficiency of the heart and to create *p*-*V*-diagrams, a realistic pressure distribution in the heart is essential. This requires instationary pressure boundaries. Starting from an existing arterial circulation model, developed at the Institute of Industrial Information Technology (IIIT), University of Karlsruhe, a linearised circulation model for the arterial system was created. Additionally, a venous circulation model and a circulation model for the lung were developed and used to calculate the unsteady boundary conditions for the simulations. The results will be presented in this paper.

Introduction

Heart diseases statistically have been the number one cause of death in Germany during the past years. Next to cardiac transplantation, surgical reconstruction of dilated ventricles is becoming an important alternative. Within the international STICH- (Surgical Treatment of Ischemic Heart Failures) trial one possible operation method (DOR-method) is tested. In cooperation with a member of this study, the university hospital in Freiburg, the Institute for Fluid Mechanics, University of Karlsruhe, is developing KAHMO (KArlsruhe Heart MOdel), a patient specific model of the human heart [1]. The aim of this project is to create a tool for planning and improving heart surgery procedures.

Using this model, numerical simulations of the pulsatile flow in a pumping human ventricle were performed. The pulsatile flow structure and quantification of losses were analysed. The movement of the human ventricle was obtained by segmentation of Magnetic Resonance Images (MRI) and prescribed in the simulation.

Blood was regarded incompressible and simulations were carried out with a very simple circulation model that causes an unrealistic pressure level in the ventricle. Due to incompressibility, the pressure level has no influence on the pulsatile flow itself. But to determine the losses or a pressure-volume (*p*-*V*)-diagram, a correct pressure level is a precondition. To realise a correct pressure level, realistic instationary pressure boundaries have to be used in the simulations. Therefore, a new circulation model had to be implemented in the existing model. The aim was to develop a multi-scale model (3D-Flow-Simulation coupled with a 1D circulation model) which provides time-depending pressure boundaries for the 3D-Flow-Simulation. Starting from an existing circulation model of the arterial system [2], currently in clinical trial, the model was linearised and transformed to a state space representation. A model for the venous blood flow and the blood flow through the lung was added.

Materials and Methods

The simulations of the human heart were performed using the three dimensional, incompressible and instationary continuum mechanical conservation equations for mass (1) and momentum (2) (Navier-Stokes-Equations):

$$\nabla \cdot (\rho \cdot \vec{v}) = 0 \quad (1)$$

$$\rho \cdot \left(\frac{\partial \vec{v}}{\partial t} + (\vec{v} \cdot \nabla)\vec{v} \right) = \vec{F} - \nabla p + \mu \cdot \Delta \vec{v} \quad (2)$$

These equations are solved on a three dimensional discrete calculation grid by commercial CFD (STAR-CD) based on the arbitrary Lagrange Euler formulation (ALE) of the finite volume method (FVM).

The ventricular geometry is prescribed by segmentation from MRI recording sets, generation of topologically identical grids for each MRI trigger step and approximation between these grids. The approximation is done by a third order Bezier-Spline. The movement of the walls taken from the MRI is a boundary condition. The influence of the flow on the geometry is neglected. The heart valves are modelled as a simplified two-dimensional valve with time variable resistance.

Most biomedical simulations only consider a part of a whole system. But this part has to be regarded as being connected to the complete system to get realistic results. Thus, boundary conditions are needed on every edge of the simulation to solve the numerical equations. Using the

ISSN: 1727-1983

correct boundary conditions is very important to get reliable results from the simulation. The choice of the boundary conditions affects the entire simulation and the calculation in the evaluated area. Using the wrong boundary conditions will still lead to mathematically (and perhaps even physically) correct results. But these results will not display the real conditions.

Figure 1 shows the numerical KAHMO model of the left human ventricle. The simulation volume ends upstream at the beginning of the inlet tube and downstream at the A. carotis, A. brachiocephalicus., A. subclavia sinistra and the end of the aorta. Here, realistic boundary conditions in terms of time dependent pressure values are required for the human heart simulations. To obtain these

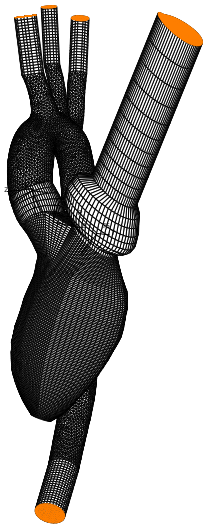

Figure 1: Numerical model of the human left ventricle and aorta (KAHMO) with boundaries

pressure values, a model of the human circulation system is needed. But the overall calculation time has to be kept inside a reasonable time frame.

The Institute of Industrial Information Technology (IIIT) has developed a mathematical model of the human arterial circulation system [2] consisting of 130 segments. It represents a detailed anatomically correct systemic arterial tree in which each segment is represented by a thin-walled cylindrical tube. Specified mechanical properties (length, diameter, wall thickness, Young's modulus) were assigned to each vessel segment. The starting point for the development of this model are the mass conservation equation (3) and the Navier-Stokes-Equations (4) for a cylindrical coordinate system.

$$\frac{\partial \rho}{\partial t} + \frac{\partial(\rho \cdot r \cdot v_r)}{r \cdot \partial r} + \frac{\partial(\rho \cdot v_\varphi)}{r \cdot \partial \varphi} + \frac{\partial(\rho \cdot v_z)}{\partial z} = 0 \qquad (3)$$

$$\rho \cdot \left[\frac{\partial v_r}{\partial t} + \frac{v_r \cdot \partial v_r}{\partial r} + \frac{v_\varphi \cdot \partial v_r}{r \cdot \partial \varphi} - \frac{v_\varphi^2}{r} + \frac{v_z \cdot \partial v_r}{\partial z} \right] = F_r - \frac{\partial p}{\partial r} + \mu \cdot \left[\frac{\partial}{\partial r} \left(\frac{\partial (r \cdot v_r)}{r \cdot \partial r} \right) + \frac{\partial^2 v_r}{r^2 \partial \varphi^2} - \frac{2 \cdot \partial v_\varphi}{r^2 \partial \varphi} + \frac{\partial^2 v_r}{\partial z^2} \right]$$

$$\rho \cdot \left[\frac{\partial v_\varphi}{\partial t} + \frac{v_r \partial v_\varphi}{\partial r} + \frac{v_\varphi \partial v_\varphi}{r \partial \varphi} + \frac{v_\varphi v_r}{r} + \frac{v_z \partial v_\varphi}{\partial z} \right] = F_\varphi - \frac{\partial p}{r \partial \varphi} + \mu \cdot \left[\frac{\partial}{\partial r} \left(\frac{\partial (r \cdot v_\varphi)}{r \cdot \partial r} \right) + \frac{\partial^2 v_\varphi}{r^2 \partial \varphi^2} + \frac{2}{r^2} \frac{\partial v_r}{\partial \varphi} + \frac{\partial^2 v_\varphi}{\partial z^2} \right]$$

$$\rho \cdot \left[\frac{\partial v_z}{\partial t} + \frac{v_r \cdot \partial v_z}{\partial r} + \frac{v_\varphi \cdot \partial v_z}{r \cdot \partial \varphi} + \frac{v_z \cdot \partial v_z}{\partial z} \right] = F_z - \frac{\partial p}{\partial z} + \mu \cdot \left[\frac{\partial}{r \cdot \partial r} \left(\frac{r \cdot \partial v_z}{\partial r} \right) + \frac{\partial^2 v_z}{r^2 \cdot \partial \varphi^2} + \frac{\partial^2 v_z}{\partial z^2} \right] \qquad (4)$$

With the assumptions that

- the velocity v_z is significantly smaller than the pulse wave velocity and therefore negligible: $\Rightarrow \frac{\partial}{\partial z} = 0; \quad \frac{\partial^2}{\partial z^2} = 0,$
- the radial velocity v_r is significantly smaller than the axial velocity v_z: $\Rightarrow v_r \ll v_z$ and
- pressure is almost independent of the radius

the resulting equation for an incompressible fluid in a rotationally symmetric system is:

$$\frac{\partial^2 v_z}{\partial r^2} + \frac{1}{r} \cdot \frac{\partial v_z}{\partial r} - \frac{\rho}{\mu} \cdot \frac{\partial v_z}{\partial t} = \frac{1}{\mu} \frac{\partial p}{\partial z} \qquad (5)$$

With the assumption of a Hagen-Poiseuille flow, equation (6) represents the resulting equation to calculate blood pressure in each segment. Using the vessel formula for thin pipes [3] equation (7) is the final equation for the flux:

$$-\frac{\partial p}{\partial z} = \frac{\rho \cdot \ell}{\pi \cdot r_0^2} \cdot \frac{\partial q}{\partial t} + \frac{8 \cdot \mu \cdot \ell}{\pi \cdot r_o^4} \cdot q \qquad (6)$$

$$-\frac{\partial q}{\partial z} = \frac{3 \cdot \pi \cdot r_0^3 \cdot \ell}{2 \cdot E \cdot d} \cdot \frac{\partial p}{\partial t} \qquad (7)$$

with

- ℓ = vessel length
- E = Young's modulus
- ρ = blood density
- ν = blood viscosity
- r = vessel radius
- d = thickness of the vessel wall.

These equations are similar to the equations (8) and (9) for a simple circuit (figure 2). Therefore it is pos-

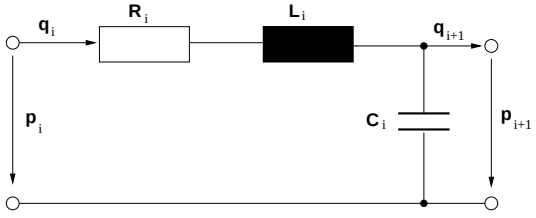

Figure 2: Electrical circuit with R, L and C implemented in the IIIT-circulation model

ISSN: 1727-1983

sible to link flow and pressure with terms of resistance (R), inductance (L) and capacitance (C). That means that blood flow and pressure are expressed by the intensity of current (i) and voltage (U). Table 1 shows this interrelationship.

$$-\frac{\partial U}{\partial z} = L \cdot \frac{\partial i}{\partial t} + R \cdot i \quad (8)$$

$$-\frac{\partial i}{\partial z} = C \cdot \frac{\partial U}{\partial t} \quad (9)$$

Table 1: Electrical analogon for pressure p and flux q in the circulation model

Flow parameter	Electrical analogon	
Pressure p $[Pa]$	Voltage	U $[V]$
Flux q $[\frac{m^3}{s}]$	Current	i $[A]$
$\frac{8 \cdot \mu l}{\pi \cdot r^4}$	Resistance	R $[\frac{V}{A}]$
$\frac{\rho \cdot l}{\pi \cdot r^2}$	Inductance	L $[\frac{V \cdot s}{A}]$
$\frac{3 \cdot \pi \cdot r^3 \cdot l}{2 \cdot E \cdot d}$	Capacitance	C $[A \cdot s]$

Resistance, inductance and capacitance are implemented for each vessel segment according to physical properties of the arterial tree and the rheology of the blood.

A set of these vessel segments was used for the circulation model of the lungs and for the venous body circulation model. But the complexity of the existing model for the arterial tree is too high to use it as a boundary condition in the heart simulation. As a consequence, the number of the input quantities as well as the number of the segments had to be decreased. It had to be evaluated how the 130 vessel segments can be merged and which outputs will be needed for the flow simulations. The 130 segments have been combined into eight collective parts. These parts have been transferred into state space separately. Thus, every single part is no longer composed of a number of elements but is described by the matrices $\underline{A}$, $\underline{B}$, $\underline{C}$ and $\underline{D}$:

$$\dot{\vec{x}} = \underline{A}\vec{x} + \underline{B}\vec{u} \quad (10)$$

$$\vec{y} = \underline{C}\vec{x} + \underline{D}\vec{u} \quad (11)$$

with:

- $\vec{x}$ = state vector (n by 1)
- $\vec{y}$ = output vector (m by 1)
- $\vec{u}$ = input (or control) vector (p by 1)
- $\underline{A}$ = state matrix (n by n)
- $\underline{B}$ = input matrix (n by m)
- $\underline{C}$ = output matrix (p by n)
- $\underline{D}$ = feedthrough (or feedforward) matrix (p by m)

The matrices $\underline{A}$, $\underline{B}$, $\underline{C}$ and $\underline{D}$ determine the relationships between the state and input and output variables. The single parts have been connected to form a new circulation model for the arterial tree. Instead of solving two differential equations for every single segment for each time step, there are just two equations in eight parts left. This circulation model (linearised KAHMO circulation model) of the arterial tree is now defined by 32 matrices (four for each of the eight parts).

Providing the simulation model of the human heart with the necessary boundaries a complete circulation model was required. Based on previous experiences models of the venous body circulation and of the circulation in the lung were developed. A set of the original segments of the arterial circulation model was used for both. Therefore the mechanical properties length, diameter, wall thickness and Young's modulus have to be determined in these models. These parameters have been adjusted with in vivo measurement curves from literature ([4], [5], [6]). The complete circulation model was realised using the MATLAB toolbox Simulink.

Results

In a first step the linearised KAHMO circulation model was evaluated by comparing the calculated pressures at the A. carotis, A. brachiocephalicus., A. subclavia sinistra and the end of the aorta with the results from the original circulation model (IIIT). Both circulation models depend on the flux through the aortic valve as input data. Two of the used fluxes are shown in figure 3.

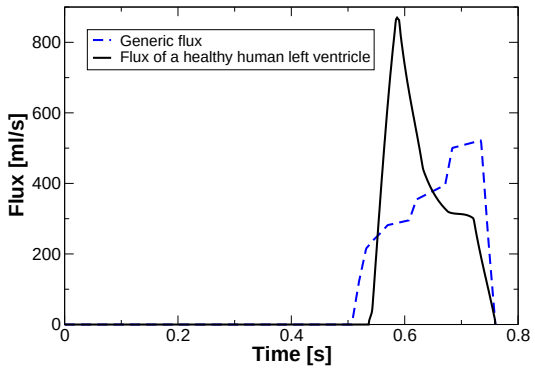

Figure 3: Blood flux through the aortic valve for a generic and a healthy human heart

The generic flux (figure 3) was used in the developing process of the linearised KAHMO circulation model. The other one is the flux through the aortic valve resulting from a ventricular simulation of a healthy human heart.

Both circulation models produce data sets representing the pressure behind the aorta and the three branches. The comparison between the original arterial circulation model [2] and the linearised KAHMO circulation model

ISSN: 1727-1983

using the generic flux shows a difference in the pressure outputs of only one percent. Figure 4 and 5 show the differences in the pressure distribution at the A. carotis (figure 4) and at the end of the aorta (figure 5) between the original model and the linearised KAHMO circulation model.

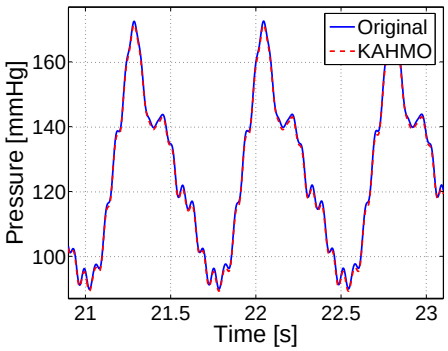

Figure 4: Differences between the pressure distributions in the A. carotis with the generic flux as input data

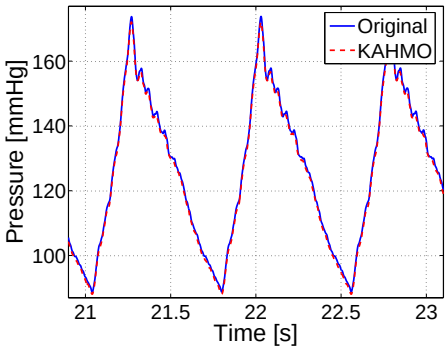

Figure 5: Differences between the pressure distributions at the end of the aorta with the generic flux as input data

Using the flux resulting from the simulation of a patient specific human heart, the KAHMO circulation model corresponds very well with the results of the original model (figure 6 and figure 7).

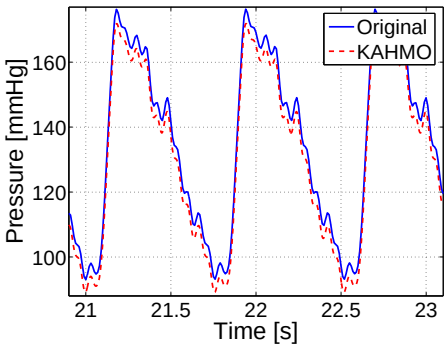

Figure 6: Differences between the pressure distributions in the A. carotis with the flux of a simulated healthy human heart

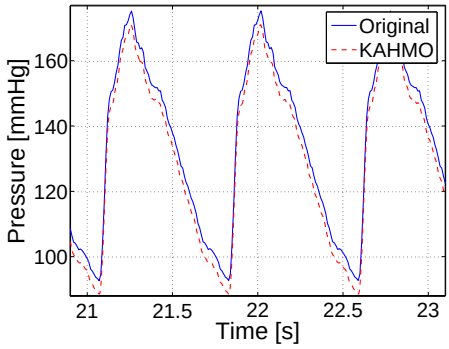

Figure 7: Differences between the pressure distributions at the end of the aorta with the flux of a simulated healthy human heart

After these preliminary investigations an interface in terms of a STAR-CD user subroutine was implemented to connect the linearised KAHMO circulation model as well as the circulation model of the lung with the heart simulations.

The resulting flow pattern for simulations with and without a circulation model is shown in figure 8. The flow pattern is identical and the KAHMO circulation model has, as predicted, no effect on them.

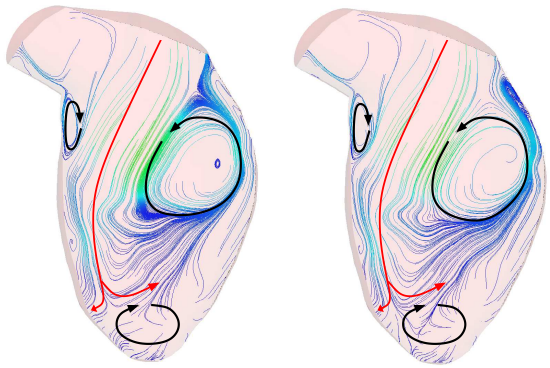

Figure 8: Flow pattern in the left ventricle. *left*: without circulation model; *right*: with circulation model

The *p*-*V*-diagram in figure 9 shows the filling of the left ventricle ① along the rest expansion curve, the iso-

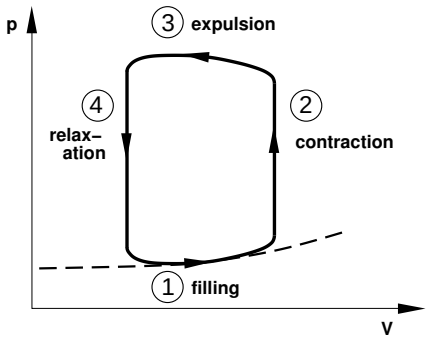

Figure 9: *p*-*V*-diagram in the left ventricle during one cardiac cycle [7]

ISSN: 1727-1983

volumetric contraction ②, as well as the expulsion ③ and the isovolumetric relaxation ④. The enclosed surface is the systolic work done by the left ventricle.

Figure 10 shows the *p-V*-diagram as the result of a heart simulation without a circulation model, figure 11 the significantly improved *p-V*-diagram which results from a simulation with the KAHMO circulation model and the circulation model for the lung as boundary conditions for the heart simulation.

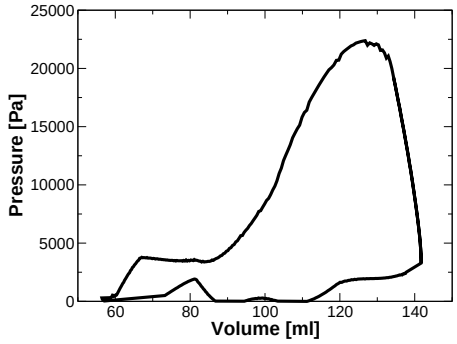

Figure 10: *p-V*-diagram as the result of a simulation without the circulation model

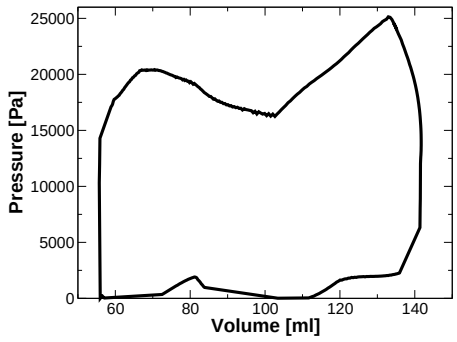

Figure 11: *p-V*-diagram as the result of a simulation with the circulation model

Discussion

The generic flux through the aortic valve (figure 3) was used during the reduction of the vessel segments and the linearisation to generate each single part. Thus, there had to be very small differences in the pressure outputs between the orginal model (IIIT) and the KAHMO circulation model (one percent, figure 4 and 5). For further validation new data sets were used. These data sets of the aortic flux were taken from records of heart simulations. Figure 3 shows a flux through the aortic valve which resulted from a simulation of patient specific human heart. But even with variations in the input data sets, as shown in figure 3, the difference between the original circulation model and the linearised KAHMO circulation model is only three percent. Thus, the KAHMO circulation model is able to provide realistic boundary conditions for the 3D simulations of human hearts.

In the simulation without a circulation model the isovolumetric contraction and relaxation were not included. The resulting *p-V*-diagram (figure 10) shows big differences to *p-V*-diagrams shown in literature ([4], [5], [6]). Using the linearised KAHMO circulation model and the circulation model for the lung the simulation is provided with realistic boundary conditions. Therefore, the *p-V*-diagram (figure 11) out of this simulation displays the isovolumetric contraction as well as the isovolumetric relaxation. Nevertheless, comparing figure 9 with figure 11 there is an obvious difference during the systole (expulsion, ③ in figure 9). The reason for this difference has to be investigated further.

Conclusions

The flow structure inside a pumping heart can be calculated with a state of the art Navier-Stokes-FVM approach. Using the linearised KAHMO circulation model and the circulation model of the lung instead of constant pressure boundaries has no effects on the flow pattern in the heart. But it is absolutely necessary to determine the losses and the *p-V*-diagram for each individual simulated human heart. The KAHMO circulation model provides realistic pressure boundaries for the simulations. With the presented KAHMO circulation model it was possible to improve the *p-V*-diagram for simulated human hearts.

References

[1] OERTEL, H. Modelling the human cardiac fluid mechanics. Technical report, 2005.

[2] MEYROWITZ, G. *Automatisierung der Herz-Lungen-Maschine*. PhD thesis, Institute of Industrial Information Technology, University of Karlsruhe (TH), 2005.

[3] WITTENBURG, J. and PESTEL, E. *Festigkeitslehre : Ein Lehr- und Arbeitsbuch 3. Aufl.* Springer-Verlag, 2001.

[4] NETTER. F. *Farbatlanten der Medizin, Bd.1, Herz.* Thieme Verlag, 1990.

[5] SILBERNAGL, S. and DESPOPOULOS, A. *Taschenatlas der Physiologie*. Thieme Verlag, 2001.

[6] THEWS, G., MUTSCHLER, E., and VAUPEL, P. *Anatomie, Physiologie, Pathophysiologie des Menschen*. Wissenschaftliche Verlagsgesellschaft mbh Stuttgart, 1999.

[7] OERTEL, H. *Prandtl's Essentials of Fluid Mechanics*. Springer-Verlag, 2004.

ISSN: 1727-1983